# Reaction-Induced Cluster Ripening and Initial Size-Dependent Reaction Rates for CO Oxidation on Pt$_n$/TiO$_2$(110)-(1×1)

Simon Bonanni, Kamel Aït-Mansour, Wolfgang Harbich, and Harald Brune*

Institute of Condensed Matter Physics, Ecole Polytechnique Fédérale de Lausanne (EPFL), CH-1015 Lausanne, Switzerland

ABSTRACT: We determined the CO oxidation rates for size-selected Pt$_n$ ($n \in \{3,7,10\}$) clusters deposited onto TiO$_2$(110). In addition, we investigated the cluster morphologies and their mean sizes before and after the reaction. While the clusters are fairly stable upon annealing in ultrahigh vacuum up to 600 K, increasing the temperature while adsorbing either one of the two reactants leads to ripening already from 430 K on. This coarsening is even more pronounced when both reactants are dosed simultaneously, i.e., running the CO oxidation reaction. Since the ripening depends on the size initially deposited, there is nevertheless a size effect; the catalytic activity decreases monotonically with increasing initial cluster size.

Pt$_3$/TiO$_2$(110)
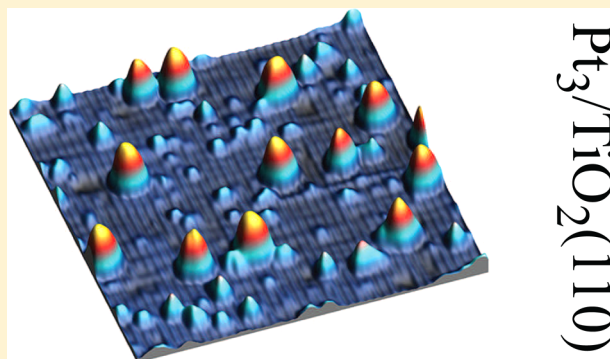
INTRODUCTION

It is well established that small metal clusters have physical and chemical properties distinctively different from those of the bulk. While the properties change rather smoothly in the so-called scalable size regime, each additional atom can substantially change the properties of interest in the non-scalable size range.[1] Metal clusters of well-defined size, shape, and composition, supporting on metal oxide surfaces, provide model catalysts that offer a fundamental understanding of the processes taking place in real catalysts via structure–reactivity correlation at the molecular level.[2] This has been shown for the smallest clusters in numerous examples, three decades ago in the famous photographic experiment by Fayet et al.,[3] and more recently in the work of Heiz et al. for metal clusters on MgO(100)[4–9] and of Anderson et al.,[10,11] Watanabe et al.,[12] and our group[13] for metal clusters on rutile TiO$_2$(110). In all these examples, size-selected cluster deposition was employed in order to prepare monodispersed supported clusters which are difficult to obtain by conventional preparation methods. We note that experiments with a finite cluster size distribution also make it possible to study size effects in the scalable regime by varying the mean cluster size.[14] However, to firmly associate a catalytic property with a certain size, one has to probe the cluster morphology not only before but also after the reaction. This information is essentially lacking in most of the experiments cited above.

It is fairly well accepted that metal catalysts deactivate, in particular under reaction conditions, as a consequence of morphological changes of the supported clusters, and that this change depends on the cluster size and cluster–support interaction.[2,15–24] This argument is even more important when the smallest entities, with only a handful of atoms, are under investigation. Accordingly, not only in model catalysts with well-defined initial conditions but also in real catalysts, this

stability under the reaction conditions sets a clear limitation to the minimum cluster size that can be reasonably employed.

Here we present a systematic study of the initial size-dependent reactivity and of the thermal as well as chemical stability of very small Pt clusters on rutile TiO$_2$(110)-(1×1) in a weak reduction state.

EXPERIMENTAL SECTION

The experiments were performed in an ultrahigh vacuum (UHV, $p_{tot} \leq 1 \times 10^{-10}$ mbar) chamber combining size-selected cluster deposition, low-temperature scanning tunneling microscopy (STM), and catalytic activity measurements with a highly sensitive detector.[25,26]

Clean TiO$_2$(110) surfaces were prepared in UHV by repeated cycles of Ar$^+$ sputtering (1 kV, 13 μAh, 300 K) and annealing at 950 K for 15 min. This procedure is known to preferentially remove oxygen,[27] leading to TiO$_{2-\delta}$ crystals with a slight oxygen deficiency.[28] This non-stoichiometry results in surface and bulk oxygen vacancies (O$_{vac}$), as well as in interstitial titanium Ti$_3^+$.[28–30] The crystal reduction state δ strongly influences the reactivity of adsorbed metal clusters.[13] This is reflected in the surface O$_{vac}$ concentration that is determined by STM.[13,31,32] Since the reduction state of the crystal changes during the course of several sample preparations, and in order to compare the strength of its effect with the initial size effect we are after, the cluster deposition experiments were carried out in the sequence Pt$_{10}$→Pt$_7$→Pt$_3$→Pt$_3$→Pt$_7$; i.e., we repeated Pt$_3$ in the fourth sample and then came back to Pt$_7$ in the fifth in order to compare with the same size studied on a less reduced substrate in sample 2. The O$_{vac}$ concentration is given in monolayers (ML); 1 ML is one vacancy per TiO$_2$(110)-(1×1) unit cell and corresponds to a density of 5.2 × 10^{14} cm^{-2}. The first TiO$_{2-\delta}$(110) sample of this sequence had 0.04 ML O$_{vac}$ and the last 0.06 ML.

The cluster source is based on sputtering of a metal target by 20 keV Kr$^+$.[33] Cluster cations are extracted, energy filtered, and mass selected by a quadrupole. The ionized particles are directed to the

as deposited

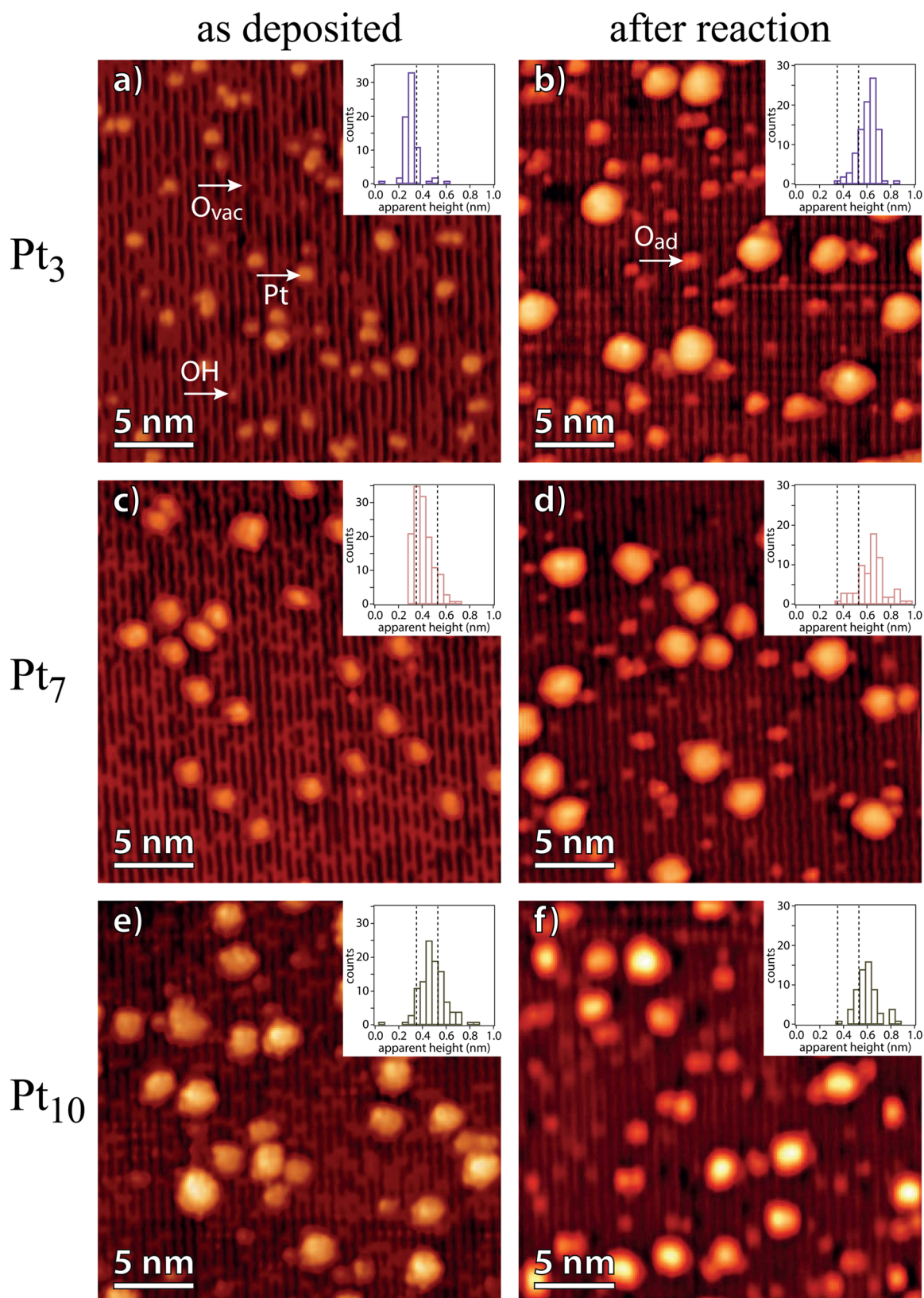## after reaction

Figure 1. STM images of size-selected Pt_3 (a,b), Pt_7 (c,d), and Pt_{10} (e,f) on $TiO_2(110)$-(1×1) as deposited (left) and after catalytic reaction (right) with exposure to CO and O_2 up to a surface temperature of 600 K. The insets show apparent height distributions.

surface whose potential defines the kinetic energy of deposition held at 7 eV/atom for all sizes investigated. This energy is a compromise between the optimum kinetic cluster energy for the quadrupole and soft landing conditions.[34] We adjusted the cluster density to obtain an overall Pt coverage of 0.02 ML, where 1 ML here is defined as an atomic density of Pt(111) of 1.5×10^{15} atoms/cm². The Pt coverage is obtained from the cluster current density times the deposition time and the cluster size. The clusters were deposited at room temperature,

and typical cluster currents were 550 pA for Pt_3, 230 pA for Pt_7, and 200 pA for Pt_{10} on a sample surface of 0.25 cm^2.

The catalytic activity of the samples was measured by recording the CO_2 signal while dosing alternating pulses of the reactants CO and O_2 into a confined volume right in front of the sample surface.[26] In order to increase the selectivity with respect to molecules from the residual gas, we dosed $^{18}O_2$ and $^{13}C^{16}O$ and detected $^{13}C^{18}O^{16}O$. Each of the pulses corresponded to an exposure of the sample to 0.08L (langmuir) CO (where $1L = 1.33 \times 10^{-6}$ mbar·s) and 0.7L O_2. Each pulse sequence lasted 10 s, and the sample temperature was increased from 300 to 600 K at a rate of 1 K/s, thus over 30 pulses. This enables to determine the CO_2 reaction rate as a function of sample temperature for each of the deposited cluster sizes.[13]

STM images were taken directly after cluster deposition and after exposure to the reactants. Comparison of the respective cluster densities and apparent heights allowed us to detect cluster ripening and morphology transformations induced by the adsorption and reaction enthalpy, respectively. The apparent cluster height histograms were obtained by analyzing ~200 clusters per sample. The STM images were recorded in constant current mode at $V_t = 1.5$ V and $I_t = 100$ pA at a temperature of 80 K.

■ RESULTS

STM images after deposition of Pt_3, Pt_7, and Pt_{10} are shown in the left-hand column of Figure 1. In agreement with the literature,[13,28] the $TiO_2(110)$ terraces display parallel bright and dark stripes corresponding to titanium atom rows and bridging oxygen atom rows of the un-reconstructed surface. The atomic steps (not shown) have an apparent height of 3.2 Å, and the shallow protrusions on the dark lines are O_{vac}.[13] In addition, the terraces exhibit very few OH groups as a consequence of water dissociation from the residual gas.[13,35] The larger features correspond to Pt clusters. Their apparent size (height as well as width) clearly increases from Pt_3 to Pt_{10}. The clusters are not all imaged in the same way. This is mostly due to different conformations of the same size. Cluster fragmentation and coalescence by cluster diffusion would give rise to a polydisperse size distribution that would also be imaged in a non-uniform way. However, cluster diffusion is absent at 300 K, as concluded from the fact that the clusters are equally distributed over the surface; in particular, there is no accumulation at substrate steps. Fragmentation is judged to be negligible on the basis of the cluster densities agreeing for all three sizes very well with the ones expected from the respective cluster currents and deposition times.

From the histograms shown as insets, one can infer that the great majority of Pt_3 has an apparent height reminiscent of one atomic Pt layer (0.35 nm).[36] Most of the Pt_7 clusters are also one atomic layer high; however, there is a clear tail toward double-layer height that is absent for Pt_3. Pt_{10} clusters have a symmetric histogram centered at double-layer height, with equal weights on single- and triple-layer apparent heights. These apparent height distributions are in excellent agreement with the ones reported by Isomura et al.[36] These authors deposited atoms in the soft landing regime with a kinetic energy of 1.2 eV/atom.[34] Hence, this agreement further supports our conclusion of cluster fragmentation and diffusion being negligible.

The right-hand column of Figure 1 shows the surface after catalytic activity measurements, i.e., after exposure of the sample to alternating pulses of the two reactants, O_2 and CO, while the temperature was increased from 300 to 600 K. From the cluster densities we infer significant coarsening. The clusters now have a mean size of 12, 14, and 16 atoms. Hence, Pt_3 ripens more than Pt_{10}, in line with the expectation of larger

clusters being more stable against both Smoluchowski and Ostwald ripening. Note also the change in the apparent height distributions. In all cases, the clusters now are mostly double layers, with the most abundant apparent height being slightly above the double layer. The apparent cluster volume increase is related to tip convolution effects, which are larger for the higher clusters.

Before discussing cluster coarsening in more detail, we focus on the reaction rate as a function of the initial cluster size and temperature. Figure 2 shows that the CO_2 production rate per
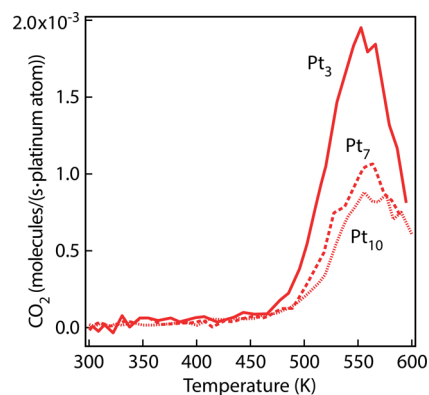

Figure 2. CO_2 production rates per Pt density as a function of deposited cluster size and temperature.

Pt atom is highest for an initial size of 3 atoms. Albeit the mean size on which the reaction takes place increases during the temperature ramp and gas exposure, there is a clear initial size dependence, since this coarsening depends on the initial size. The CO_2 production rate is essentially given by the CO adsorption and desorption kinetics. We find that CO blocks the oxygen dissociation and thereby the reaction below 470 K, as in a real catalyst, and the temperature profiles of the reaction rates are compatible with thermal desorption spectra of CO desorbing from Pt nanoparticles.[37] In addition to the reaction rates, also the temperatures at which these rates reach their respective maximums show an initial size dependence. The temperature is largest for Pt_{10}, which is expected since CO is slightly more strongly bound to larger Pt clusters.

Figure 3 shows the maximum reaction rates as a function of $n^{-2/3}$, where n is the initial size. One sees a linear behavior with an intercept at 0. If we assume, in a crude model, the cluster volume to be proportional to n, the surface to $n^{2/3}$, and the perimeter to $n^{1/3}$, we find the relative length-to-volume ratio to depend on $n^{-2/3}$. The perimeter-to-volume ratio has to go to zero for large clusters. Both the linearity and the interception are reflected in the measurements. Note that no other scaling like the surface-to-volume ratio which goes with $n^{-1/3}$ is represented by the experimental data. We take this as an indication that O_2 dissociates at the low-coordinated perimeter sites. This has been found, for example, in calculations for Au clusters but not for Pt clusters on titania.[38] One also recognizes the spread of the data as a function of the sample reduction state. The sequence of points was Pt_{10}, Pt_7, Pt_3, all shown in black, followed by Pt_3 and Pt_7, both shown in red. The first sample had 0.04 ML O_{vac} and the last 0.06 ML. In agreement with our previous work,[13] the reaction rates go down with increasing surface O_{vac} density; however, the initial size effect is independent of the substrate reduction state.
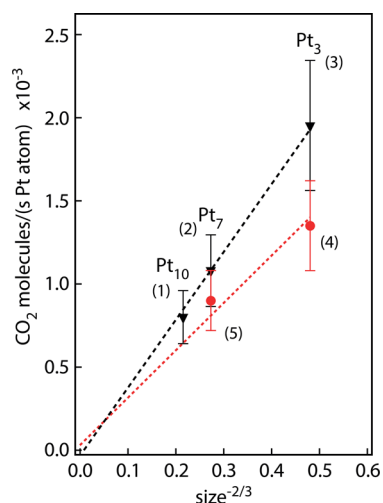
Figure 3. CO_2 production rates per Pt atom as a function of $n^{-2/3}$ (where n is the initial size), showing in addition to the initial size effect the evolution with substrate reduction state that increases from 0.04 ML O_{vac} for the first sample ((1)Pt_{10}, black point) to 0.06 ML in the last ((5)Pt_7, red point).

In order to shed more light on the conditions that influence the cluster stability, and to understand at which size catalyst particles can operate in a stable way, we studied the morphology and size of deposited Pt heptamers as a function of temperature and gas exposure. Pt_7 clusters were deposited with a nominal platinum coverage of 0.025 ML and then annealed to the temperatures indicated on the right-hand side in Figure 4, under the conditions given in the columns of this figure, namely, under vacuum and while dosing with O_2, CO, and a 1:1 mixture of both reactants. The reactant pressure was 1×10^{-6} mbar, and the annealing time 600 s. Thereby, the exposure was more than 20 times higher than in the experiments discussed above. After the exposure/annealing, the samples were cooled to 80 K for STM measurements.
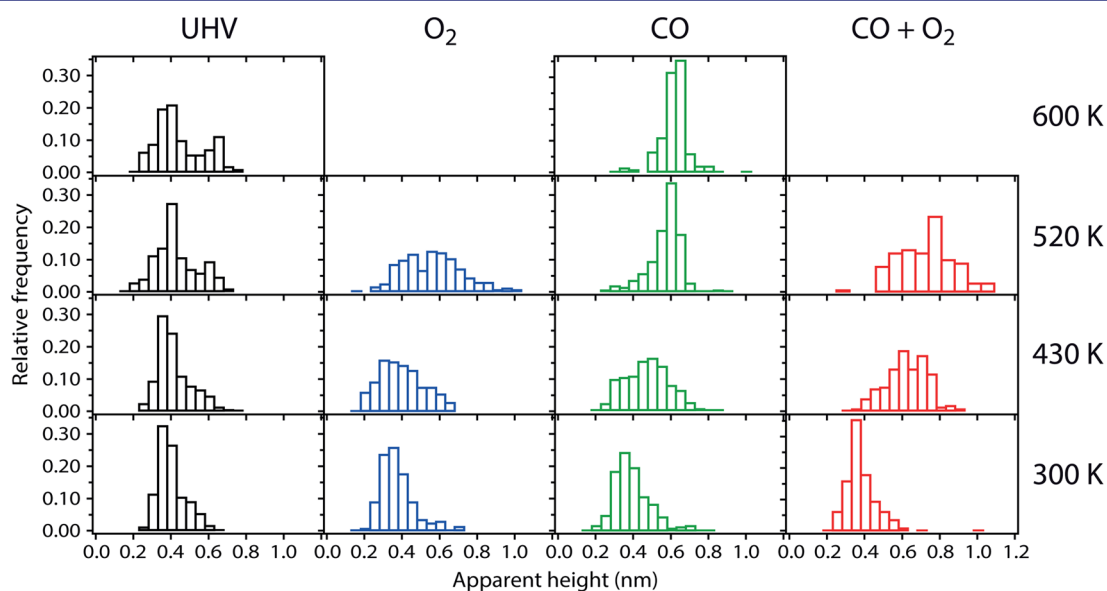
The clusters are remarkably stable against annealing in UHV. The apparent height histogram does not change until 430 K, and it changes very little at 520 K; only at 600 K annealing temperature is there a significant peak at 0.6 nm, reminiscent of double-layer height.[36] The mean cluster size of this experiment, shown in Figure 5 as a black curve, does not change until 430
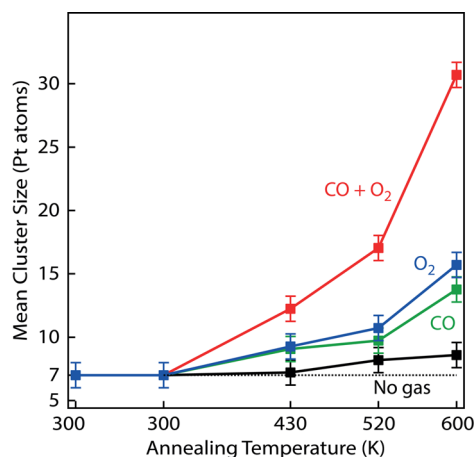

Figure 5. Mean size of deposited Pt_7 cluster after annealing in a vacuum (black) and exposure to O_2 (blue), CO (green), and both reactants (red). Conditions as in Figure 4.

K; it then increases slightly to 8.2 ± 1.0 Pt atoms per cluster at 520 K, and stays within the error bar at this value after annealing to 600 K. Exposure of the clusters to oxygen induces a significant broadening of the apparent height distribution, with bilayer clusters being most abundant and equal parts of mono- and trilayer clusters. The mean size increases already at 430 K to 10.7 ± 1.0 atoms per cluster. The same mean size is found for exposure to CO at this temperature. However, comparing the histograms, we see a clear monolayer-to-bilayer transition above 520 K, which is not the case for oxygen. Further increase of the temperature during exposure to either

Figure 4. Apparent height distributions of deposited Pt_7 clusters after annealing in UHV (black) and exposure to O_2 (blue), CO (green), and both reactants (red). Conditions: Pt coverage, 0.025 ML; annealing time, 600 s; heating rate, 2 K/s; STM measurements at 80 K; partial pressure during exposure, 1×10^{-6} mbar.

one of the reactants leads to further ripening to a mean size of ~15 atoms per cluster, while the shape of the apparent height histograms does not change markedly. STM images show in addition that, upon O_2 exposure, the Pt clusters are surrounded by a TiO_x ring;[13,39] this ring is absent for CO exposure. CO-induced morphology changes were reported for larger Pt nanoparticles and attributed to CO-assisted Ostwald ripening, i.e., to the disintegration of the supported metal particles upon the formation of surface carbonyls that transport Pt preferentially from the smaller to the larger clusters.[19,40] No transition states resulting from the disintegration of Pt clusters have been observed in our experiment. The coarsening of Pt clusters is even more pronounced under reaction conditions, i.e., when both reactants are dosed simultaneously. The histograms show a clear shift to triple-layer clusters already at 520 K, and the red curve of the mean cluster size is far above the other ones, culminating in a mean size of 30 ± 1 Pt atoms per cluster upon running the CO oxidation at 600 K. A very similar observation was made for vapor-grown Au clusters on titania[23] and larger gold clusters on TiC.[24] From the significantly greater coarsening with respect to the separate exposure to the reactants, we conclude that the excess energy of the reaction of about 2.9 eV[41] is involved in the morphology change. Hot electrons have been reported during CO oxidation on Pt nanoparticles on TiO_2.[42,43] The observed reaction-induced enhancement of coarsening can therefore proceed via an electronic excitation of the cluster substrate system.

Our findings shed new light on catalysis experiments over size-selected surface-adsorbed metal clusters. Evidently, the extent to which cluster ripening occurs depends on the cluster–substrate interaction. However, the present results encourage us to check the cluster morphology and mean size before and after the reaction of interest.

One of the first experiments on size-selected metal clusters was performed for Pt_n on MgO(100) thin films grown on Mo(100).[6] In contrast to the present study, the authors adsorbed both reactants at low temperature and used temperature-programmed reaction. They found a more or less constant CO_2 production rate up to Pt_{14}, and a sudden increase by a factor of 3 on going to Pt_{15}. This was attributed to the size-dependent ionization potential of Pt clusters matching at a given size the antibonding π_g^* orbital of oxygen. These early experiments did not investigate the cluster morphology by means of STM.

The CO oxidation rates on $Pt_n/TiO_2(110)$ were investigated under high reactant pressures and at elevated temperatures of 572−625 K.[12] These results are different from ours, as the authors reported an increase of the catalytic activity up to Pt_{7-8}, followed by a decrease until Pt_{10}, where it reached a stationary value. The reactivity increase was attributed to the transition from mono- to bilayer clusters, as observed by means of STM before the reaction. The absence of coarsening and of morphology transitions was concluded from X-ray photoelectron spectroscopy of the Pt $4f_{7/2}$ states, which showed them to have constant energy before and after the reaction. However, STM investigation of the mean cluster size and apparent height distribution after the reaction would have been a more stringent test. The difference with respect to our results can therefore be attributed to the different degree of coarsening due to the different reaction conditions, in addition to possible differences in the substrate reduction state.

■ CONCLUSION

We report size-dependent CO oxidation rates for size-selected Pt clusters on titania, correlating catalytic reactivity to cluster morphology before and after catalytic reaction measurements. We find a linear increase of this rate with the surface-to-volume ratio of atoms. In contrast to similar studies on very small size-selected clusters,[6,36] this indicates no or only a weak dependence of a size-specific electronic structure. Apart from the fact that reactivity is strongly dependent on the substrate reduction state,[13] which has been taken care of by choosing substrates of comparable reduction states, the stability of the metal clusters upon the reaction itself is an important parameter. Our measurements show a reaction-enhanced sintering which results in a final cluster size distribution different from the deposited one. This sets a minimum size limit in the study of size-selected cluster catalysis. In the case of Pt_n/TiO_2, we observe sintering during the oxidation of CO for all sizes up to the decamer, despite the Pt clusters being thermally stable in the absence of exposure to the reactants, a commonly used argument for stability. Therefore, control or at least knowledge of the cluster morphology in catalytic activity measurements is of fundamental importance.

■ AUTHOR INFORMATION

Corresponding Author
harald.brune@epfl.ch
Notes
The authors declare no competing financial interest.

■ REFERENCES

(1) Landman, U. *Proc. Natl. Acad. Sci. U.S.A.* **2005**, *102*, 6671.
(2) Gao, F.; Goodman, D. W. *Annu. Rev. Phys. Chem.* **2012**, *63*, 265.
(3) Fayet, P.; Granzer, F.; Hegenbart, G.; Moisar, E.; Pischel, B.; Wöste, L. *Phys. Rev. Lett.* **1985**, *55*, 3002.
(4) Abbet, S.; Riedo, E.; Brune, H.; Heiz, U.; Ferrari, A. M.; Giordano, L.; Pacchioni, G. *J. Am. Chem. Soc.* **2001**, *123*, 6172.
(5) Abbet, S.; Sanchez, A.; Heiz, U.; Schneider, W. D.; Ferrari, A. M.; Pacchioni, G.; Rösch, N. *J. Am. Chem. Soc.* **2000**, *122*, 3453.
(6) Heiz, U.; Abbet, S.; Sanchez, A.; Schneider, W. D. *J. Am. Chem. Soc.* **1999**, *121*, 3214.
(7) Heiz, U.; Vanolli, F.; Sanchez, A.; Schneider, W. D. *J. Am. Chem. Soc.* **1998**, *120*, 9668.
(8) Wörz, A. S.; Judai, K.; Abbet, S.; Heiz, U. *J. Am. Chem. Soc.* **2003**, *125*, 7964.
(9) Yoon, B.; Hakkinen, H.; Landman, U.; Wörz, A. S.; Antonietti, J. M.; Abbet, S.; Judai, K.; Heiz, U. *Science* **2005**, *307*, 403.
(10) Kaden, W. E.; Wu, T.; Kunkel, W. A.; Anderson, S. L. *Science* **2009**, *326*, 826.
(11) Lee, S.; Fan, C.; Wu, T.; Anderson, S. L. *J. Am. Chem. Soc.* **2004**, *126*, 5682.
(12) Watanabe, Y.; Wu, X.; Hirata, H.; Isomura, N. *Catal. Sci. Technol.* **2011**, *1*, 1490.
(13) Bonanni, S.; Aït-Mansour, K.; Harbich, W.; Brune, H. *J. Am. Chem. Soc.* **2012**, *134*, 3445.
(14) Sitja, G.; Le Moal, S.; Marsault, M.; Hamm, G.; Leroy, F.; Henry, C. R. *Nano Lett.* **2013**, *13*, 1977−1982.
(15) Fukamori, Y.; Konig, M.; Yoon, B.; Wang, B.; Esch, F.; Heiz, U.; Landman, U. *ChemCatChem* **2013**, *5*, 3330−3341.
(16) Behafarid, F.; Cuenya, B. R. *Top. Catal.* **2013**, *56*, 1542.
(17) Campbell, C. T.; Parker, S. C.; Starr, D. E. *Science* **2002**, *298*, 811.

(18) Parker, S. C.; Campbell, C. T. *Phys. Rev. B* **2007**, *75*, 035430.

(19) Berko, A.; Szoko, J.; Solymosi, F. *Surf. Sci.* **2004**, *566−568*, 337.

(20) Gao, F.; Wang, Y.; Cai, Y.; Goodman, D. W. *J. Phys. Chem. C* **2009**, *113*, 174.

(21) Simonsen, S. B.; Chorkendorf, I.; Dahl, S.; Skoglundh, M.; Sehested, J.; Helveg, S. *J. Am. Chem. Soc.* **2010**, *132*, 7968.

(22) Simonsen, S. B.; Chorkendorf, I.; Dahl, S.; Skoglundh, M.; Meinander, K.; Jensen, T. N.; Lauritsen, J. V.; Helveg, S. *J. Phys. Chem. C* **2012**, *116*, 5646.

(23) Yang, F.; Chen, M. S.; Goodman, D. W. *J. Phys. Chem. C* **2009**, *113*, 254.

(24) Ono, L. K.; Sudfeld, D.; Cuenya, B. R. *Surf. Sci.* **2006**, *600*, 5041−5050.

(25) Jödicke, H.; Schaub, R.; Bhowmick, A.; Monot, R.; Buttet, J.; Harbich, W. *Rev. Sci. Instrum.* **2000**, *71*, 2818.

(26) Bonanni, S.; Aït-Mansour, K.; Hugentobler, M.; Brune, H.; Harbich, W. *Eur. Phys. J. D* **2011**, *63*, 241.

(27) Henderson, M. A. *Surf. Sci.* **1995**, *343*, L1156.

(28) Diebold, U. *Surf. Sci. Rep.* **2003**, *48*, 53.

(29) Wendt, S.; Sprunger, P. T.; Lira, E.; Madsen, G. K. H.; Li, Z.; Hansen, J. .; Matthiesen, J.; Blekinge-Rasmussen, A.; Lægsgaard, E.; Hammer, B.; Besenbacher, F. *Science* **2008**, *320*, 1755.

(30) Yim, C. M.; Pang, C. L.; Thornton, G. *Phys. Rev. Lett.* **2010**, *104*, 036806.

(31) Lira, E.; Hansen, J. Ø.; Huo, P.; Bechstein, R.; Galliker, P.; Lægsgaard, E.; Hammer, B.; Wendt, S.; Besenbacher, F. *Surf. Sci.* **2010**, *604*, 1945.

(32) Lira, E.; Wendt, S.; Huo, P.; Hansen, J. Ø.; Streber, R.; Porsgaard, S.; Wei, Y.; Bechstein, R.; Lægsgaard, E.; Besenbacher, F. *J. Am. Chem. Soc.* **2011**, *133*, 6529.

(33) Vandoni, G.; Félix, C.; Monot, R.; Buttet, J.; Harbich, W. *Chem. Phys. Lett.* **1994**, *229*, 51.

(34) Bromann, K.; Félix, C.; Brune, H.; Harbich, W.; Monot, R.; Buttet, J.; Kern, K. *Science* **1996**, *274*, 956.

(35) Bikondoa, O.; Pang, C. L.; Ithnin, R.; Muryn, C. A.; Onishi, H.; Thornton, G. *Nat. Mater.* **2006**, *5*, 189.

(36) Isomura, N.; Wu, X.; Watanabe, Y. *J. Chem. Phys.* **2009**, *131*, 164707.

(37) Lundwall, M. J.; McClure, S. M.; Goodman, D. W. *J. Phys. Chem. C* **2010**, *114*, 7904.

(38) Rashkeev, S. N.; Lupini, A. R.; Overbury, S. H.; Pennycook, S. J.; Pantelides, S. T. *Phys. Rev. B* **2007**, *76*, 035438.

(39) Bowker, M.; Bennett, R. A. *J. Phys.: Condens. Matter* **2009**, *21*, 474224.

(40) Ouyang, R. H.; Liu, J. X.; Li, W. X. *J. Am. Chem. Soc.* **2013**, *135*, 1760.

(41) Campbell, C. T.; Ertl, G.; Kuipers, H.; Segner, J. *J. Chem. Phys.* **1980**, *73*, 5862.

(42) Ji, X. Z.; Somorjai, G. A. *J. Phys. Chem. B* **2005**, *109*, 22530.

(43) Ji, X. Z.; Zuppero, A.; Gidwani, J. M.; Somorjai, G. A. *Nano Lett.* **2005**, *5*, 753.

8707

dx.doi.org/10.1021/ja502867r | *J. Am. Chem. Soc.* 2014, 136, 8702−8707